STRUCTURAL SCIENCE
CRYSTAL ENGINEERING
MATERIALS

Volume 76 (2020)

Supporting information for article:

A new high–pressure benzocaine polymorph — towards understanding the molecular aggregation in crystals of an important active pharmaceutical ingredient (API)

Ewa Patyk-Kaźmierczak and Michał Kaźmierczak

S1. Figures

S1.1 Powder X-ray diffraction patterns

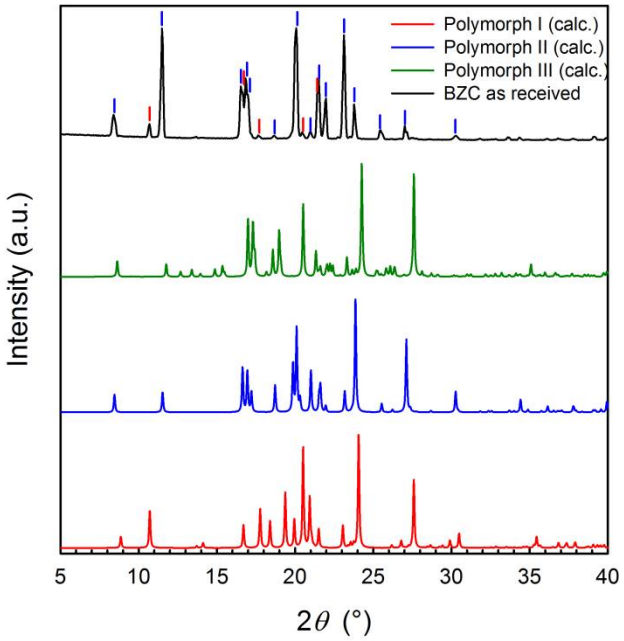

Figure S1 Experimental powder X-ray diffraction pattern for an as-received sample of BZC (black) and diffractograms calculated based on single-crystal X-ray diffraction data for BZC polymorphs I, II and III (in red, blue and green, respectively). Peaks in the diffraction pattern for as-received sample corresponding to known polymorphs of BZC are marked with ticks in colour matching specific polymorph.

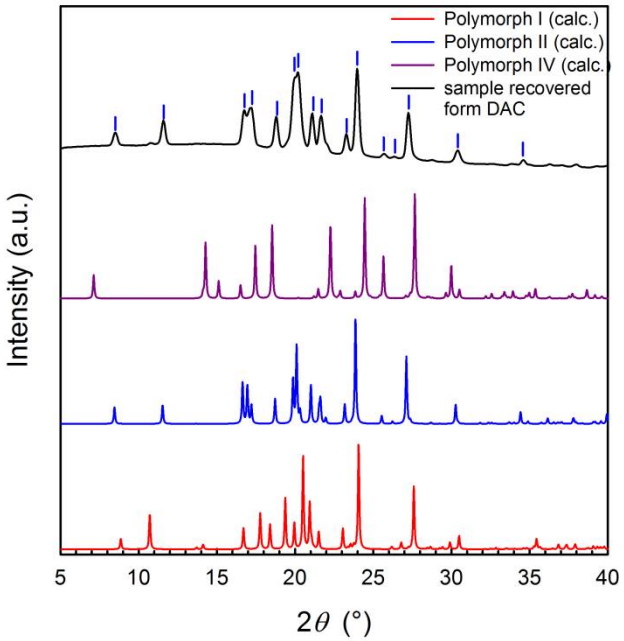

Figure S2 Experimental powder X-ray diffraction pattern for BZC sample recovered from DAC after releasing pressure from 0.60 GPa (black) and diffractograms calculated based on single-crystal X-ray diffraction data for BZC polymorphs I, II and IV (in red, blue and dark pink, respectively). Peaks in the diffraction pattern for the recovered sample corresponding to known polymorphs of BZC are marked with ticks in colour matching specific polymorph.

S1.2 High–pressure crystallisation

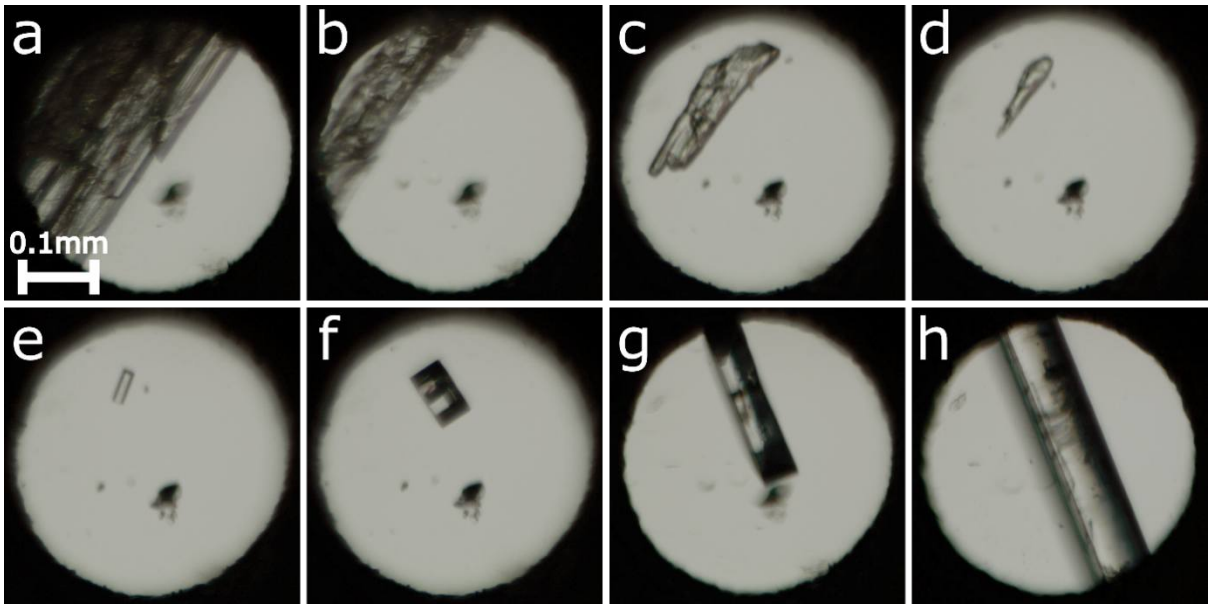

Figure S3 Stages of BZC sample dissolution (a-d) and single crystal growth (e-h) from the MeOH:EtOH:H_2O (16:3:1 vol.) solution in the DAC: (a-c) polycrystalline sample at 0.10 GPa/299 K, 0.10 GPa/320 K and 0.10 GPa/322 K, respectively; (d) single crystal at 0.10 GPa/323 K; (e) one small crystal seed at 0.10 GPa/320 K; (f,g) single crystal growth stages at 0.10 GPa and 320 and 319 K, respectively; (h) fully grown single crystal at 0.10 GPa and 293 K. Small ruby chip used for pressure measurement lies close to the centre of the chamber.

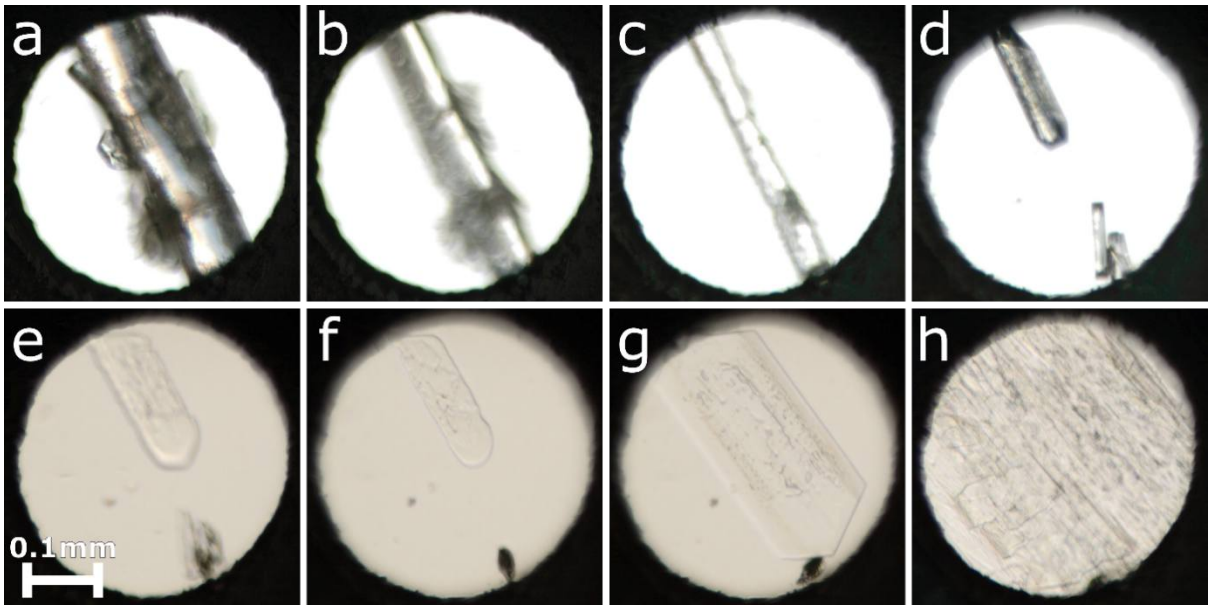

Figure S4 Stages of BZC sample dissolution (a-d) and single crystal growth (e-h) from the MeOH:EtOH:H_2O (16:3:1 vol.) solution in the DAC: (a, b) single crystal overgrown with smaller crystallites at 0.30 GPa/297 K and 0.30 GPa/339 K, respectively; (c) single crystal at 0.30 GPa/345 K; (d,e) one dominant single crystals with few smaller crystallites near the edge of the gasket at 0.30 GPa/341 K and 0.30 GPa/345K, respectively; (f,g) single crystal growth stages at 0.30 GPa and 345 and 340 K, respectively; (h) fully grown single crystal at 0.30 GPa and 299 K filling the whole chamber. The small ruby chip used for pressure measurement lies near the lower edge of the chamber.

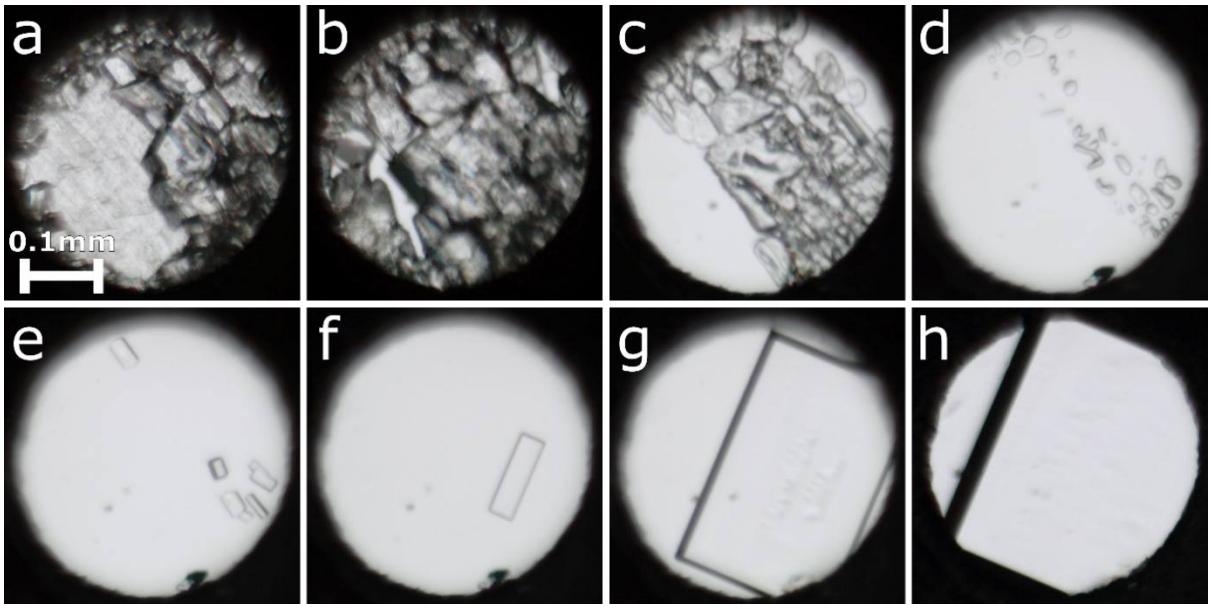

Figure S5 Stages of BZC sample dissolution (a-d) and single crystal growth (e-h) from the MeOH:EtOH:H_2O (16:3:1 vol.) solution in the DAC: (a) single crystal overgrown by polycrystalline mass at 0.55 GPa/293 K; (b) growth of the polycrystalline mass on heating of the sample at 0.55 GPa/348 K; (c) polycrystalline sample at 0.55 GPa/384 K; (d,e) few small single crystals at 0.55 GPa/395 K and 0.55 GPa/384 K, respectively; (f,g) single crystal growth at 0.55 GPa and 380 and 372 K, respectively; (h) fully grown single crystal at 0.55 GPa and 296 K. Small ruby chip used for pressure measurement lies near the lower edge of the chamber.

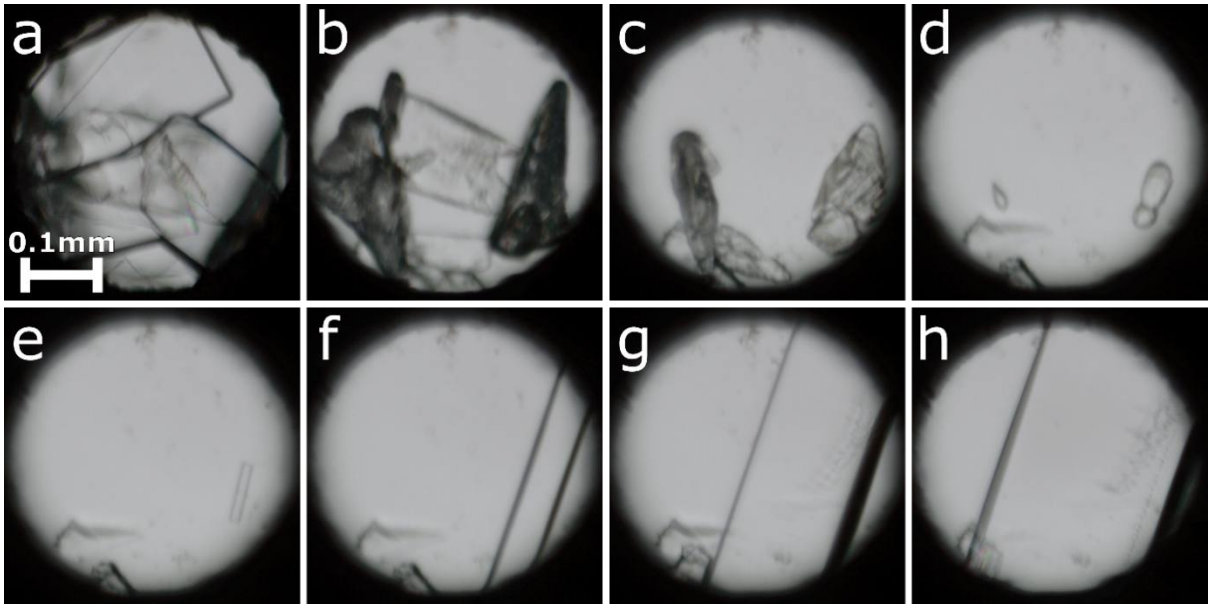

Figure S6 Stages of BZC sample dissolution (a-d) and single crystal growth (e-h) from the MeOH:EtOH:H2O (16:3:1 vol.) solution in the DAC: (a-d) few sample crystallites at pressure of 0.78 GPa and temperature of 331, 374, 390 and 395 K, respectively; (e) one small crystal seed at 0.78 GPa/382 K; (f,g) single crystal growth stages at 0.78 GPa and 371 and 360 K, respectively; (h) fully grown single crystal at 0.78 GPa and 300 K. Small ruby chip used for pressure measurement lies at the lower edge of the chamber.

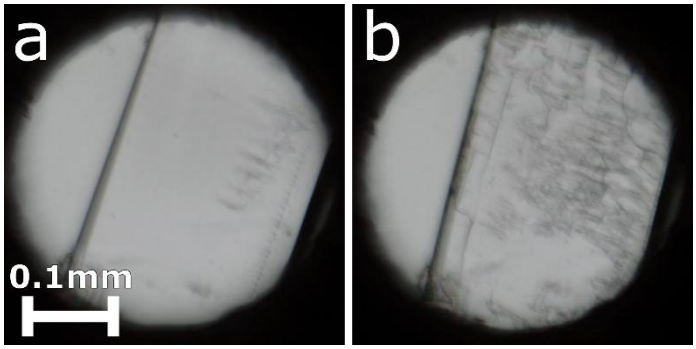

Figure S7 (a) Single crystal of BZC at 0.78 GPa and 300 K grown *in-situ* from the MeOH:EtOH:H_2O (16:3:1 vol.) solution in the DAC (see Figure S6) and (b) the same crystal after the release of pressure to 0.65 GPa. The small ruby chip used for pressure measurement lies at the lower edge of the chamber.

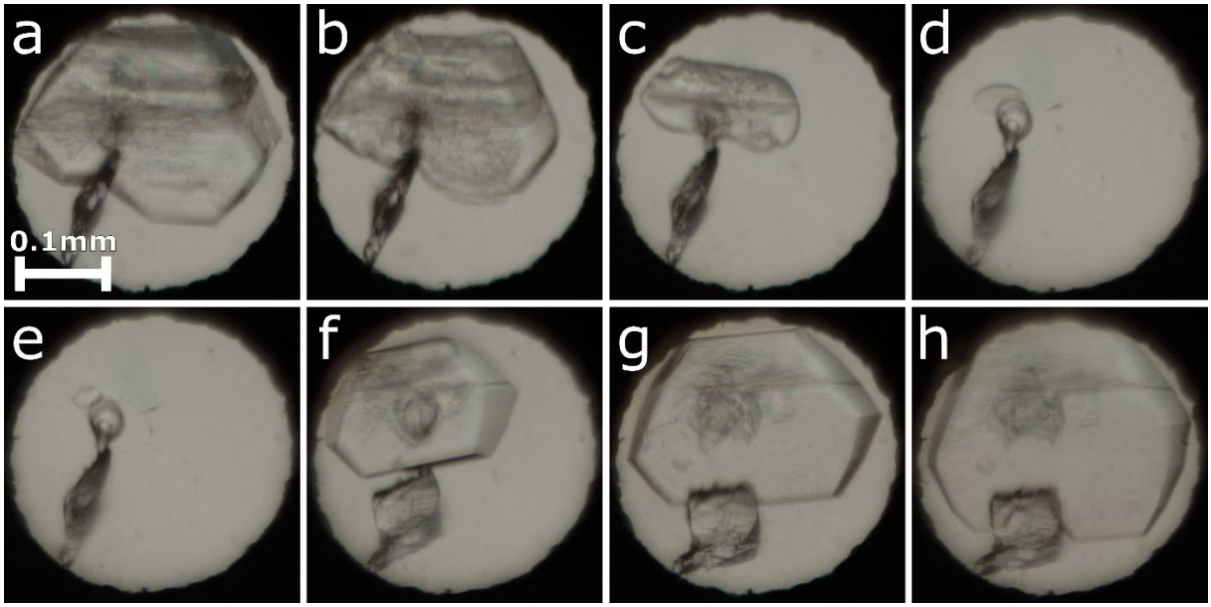

Figure S8 Stages of BZC sample dissolution (a-d) and single crystal growth (e-h) in the DAC from the 97.5% DMSO solution in water: (a-d) a single crystal at pressure of 0.41 GPa and temperature of 298, 335, 359 and 363 K, respectively; (e) one small crystal seed at 0.41 GPa/353 K; (f,g) single crystal growth stages at 0.41 GPa and 346 and 314 K, respectively; (h) fully grown single crystal at 0.41 GPa and 298 K. Ruby chip used for pressure measurement lies in the lower left part of the chamber.

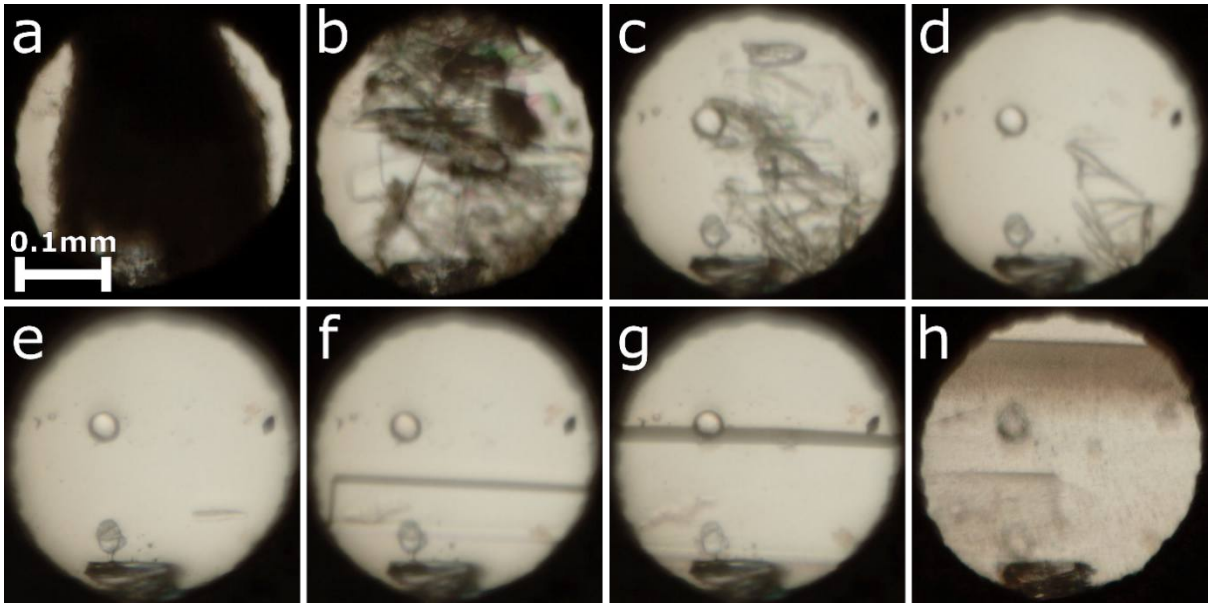

Figure S9 Stages of BZC sample dissolution (a-d) and single crystal growth (e-h) in the DAC from the 97.5% DMSO solution in water: (a-c) polycrystalline sample at pressure of 0.50 GPa and temperature of 293, 351, and 413 K, respectively; (d) few small single crystals at 0.50 GPa/422 K; (e) one small crystal seed, in the lower right part of the chamber, at 0.50 GPa/423 K; (f,g) single crystal growth stages at 0.50 GPa and 402 and 376 K, respectively; (h) fully grown single crystal at 0.50 GPa and 292 K. Ruby chip used for pressure measurement lies next to the lower edge of the chamber.

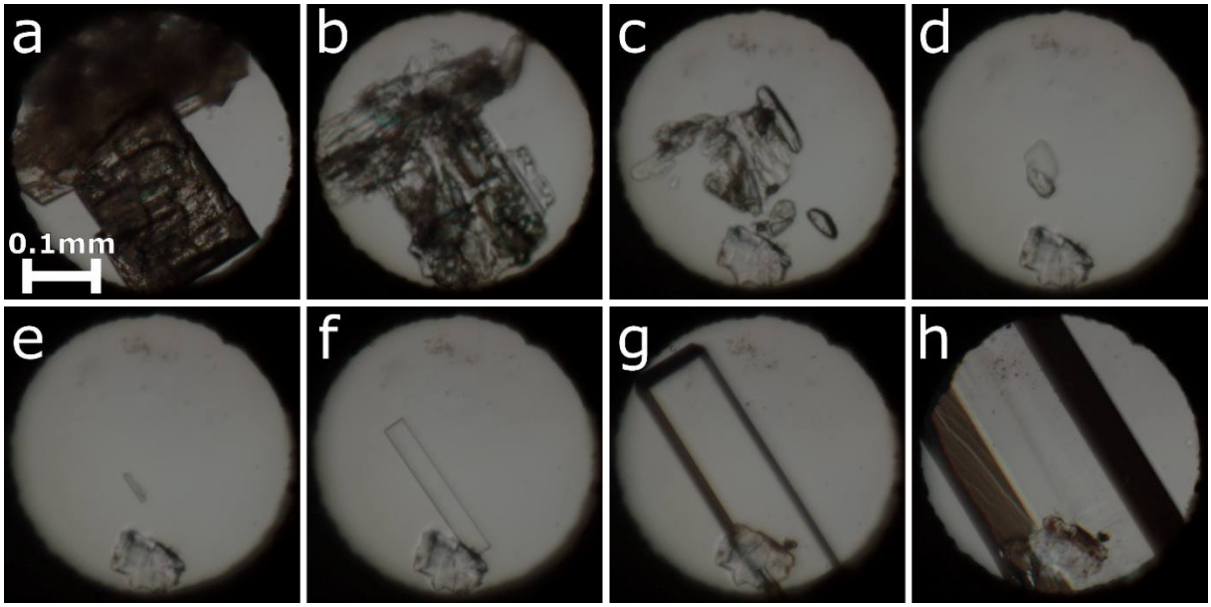

Figure S10 Stages of BZC sample dissolution (a-d) and single crystal growth (e-h) in the DAC from the 97.5% DMSO solution in water: (a-c) polycrystalline sample at pressure of 0.52 GPa and temperature of 296, 392, and 418 K, respectively; (d) two small single crystals at 0.52 GPa/417 K; (e) one small crystal seed at 0.52 GPa/406 K; (f,g) single crystal growth stages at 0.52 GPa and 401 and 394 K, respectively; (h) fully grown single crystal at 0.52 GPa and 293 K. Ruby chip used for pressure measurement lies near the lower edge of the chamber.

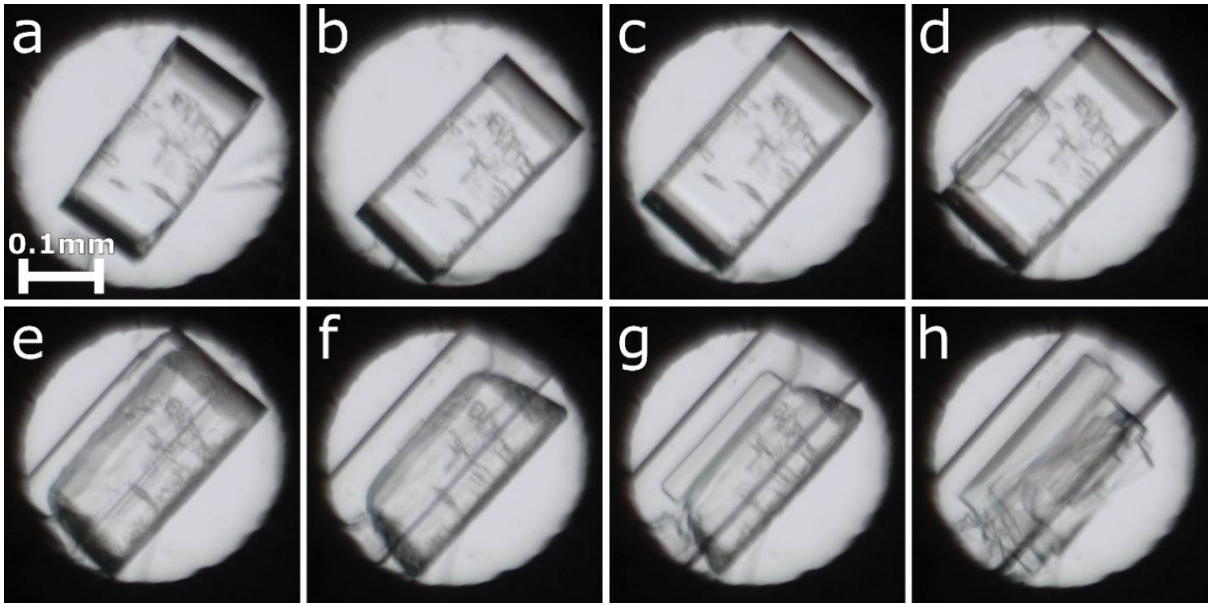

Figure S11 Stages of isothermal compression of BZC single crystal in the DAC with use of the MeOH:EtOH:H2O (16:3:1 vol.) solution as a hydrostatic medium: (a-c) sample crystal at 298 K and 0.19, 0.33 and 0.44 GPa, respectively; (d) beginning of crystallisation of BZC polymorph IV crystal at 298 K and 0.69 GPa; (e-h) gradual growth of crystals of polymorph IV and dissolution of the primary crystal at 298 K and after further increase of pressure to 0.75 GPa. Ruby chip used for pressure measurement lies near the lower-left edge of the chamber.

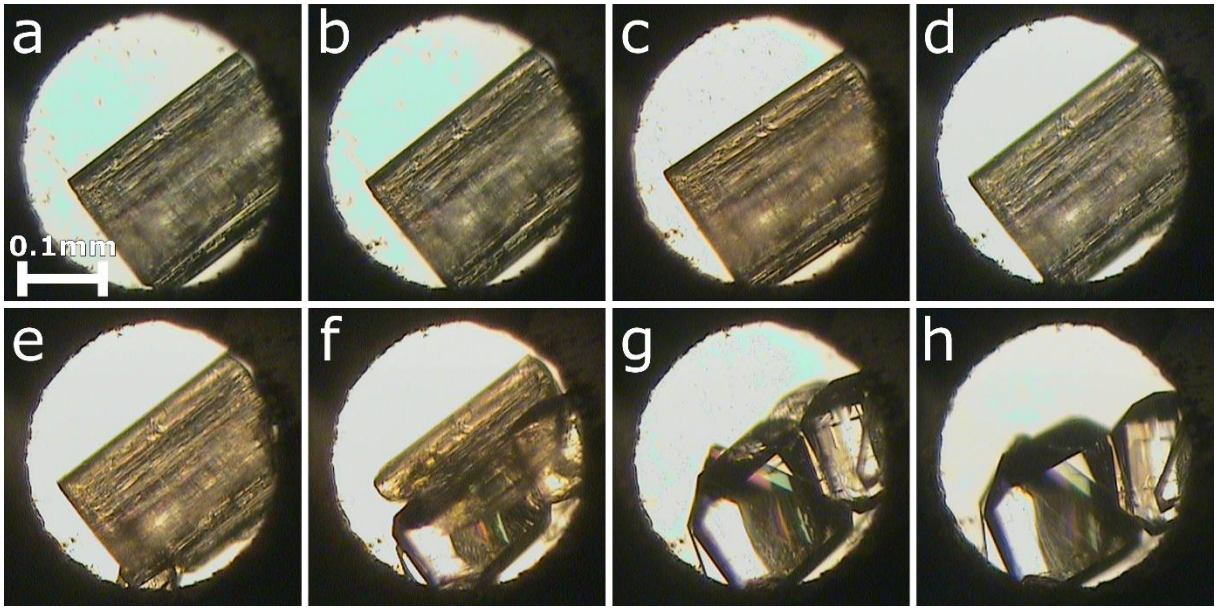

Figure S12 Stages of isothermal compression of BZC single crystal in the DAC with use of the MeOH:EtOH:H2O (16:3:1 vol.) solution as a hydrostatic medium: (a-d) sample crystal at 298 K and 0.17, 0.25, 0.53 and 0.60 GPa, respectively; (d) beginning of crystallisation of BZC polymorph IV crystal at 298 K and 0.60 GPa (small crystal can be noticed at near the lower edge of the chamber); (f-h) gradual growth of crystals of polymorph IV and dissolution of the primary crystal at 298 K and 0.60 GPa. Ruby chip is not visible due to its positioning between sample crystal and the right edge of the chamber. For a full recording of the recrystallisation process, please refer to Movie S1.

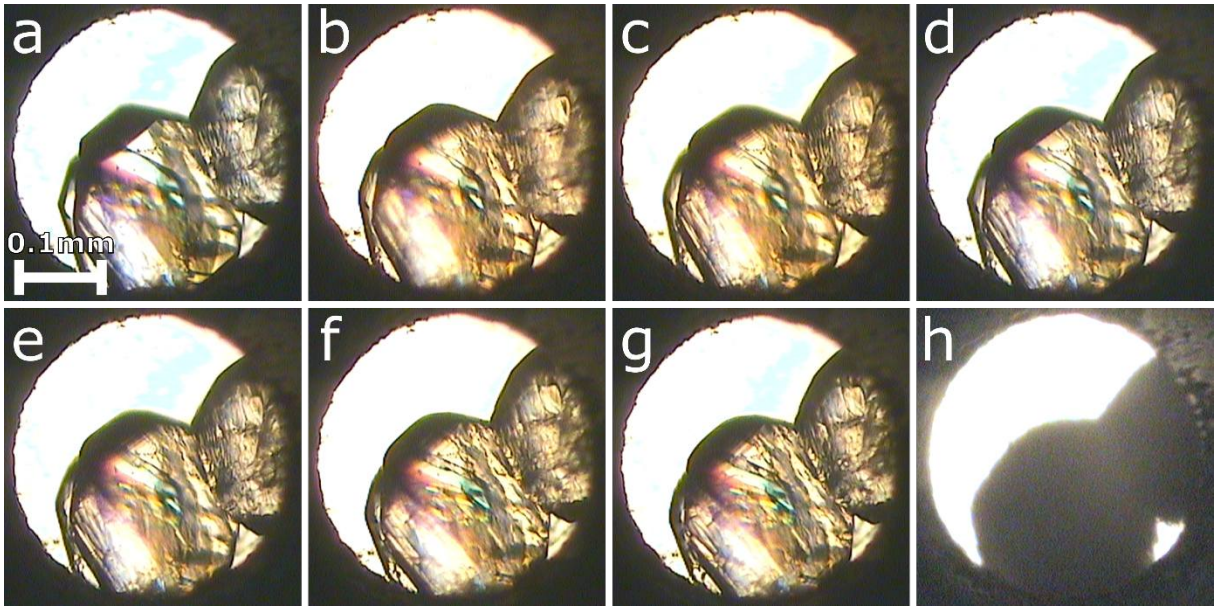

Figure S13 Changes of BZC crystals on pressure decrease. Pictures were taken at 298 K and at pressure of: (a) 0.40 GPa; (b,c) 0.43 GPa- immediately and after 7 minutes, respectively; (d,e) 0.45 GPa- immediately and after 5 minutes, respectively; (f,g) 0.37 GPa- immediately and after 10 minutes, respectively; (h) 0.18 GPa. Increase of measured pressure after loosening the DAC screws (releasing of pressure) can be associated with the partial dissolution of the crystalline sample at lower pressure affecting the density of the hydrostatic medium, and as a result, causing variation of the pressure exerted on the crystal.

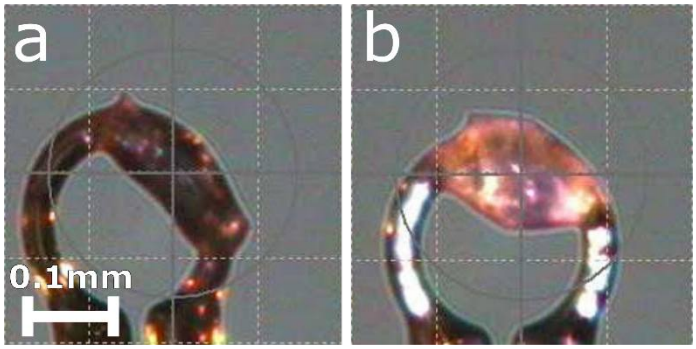

Figure S14 Single crystal (a) and polycrystalline mass (b) recovered from the DAC after decompression of crystal of polymorph IV and leaving it for 40 days.

S1.3 Intermolecular contacts

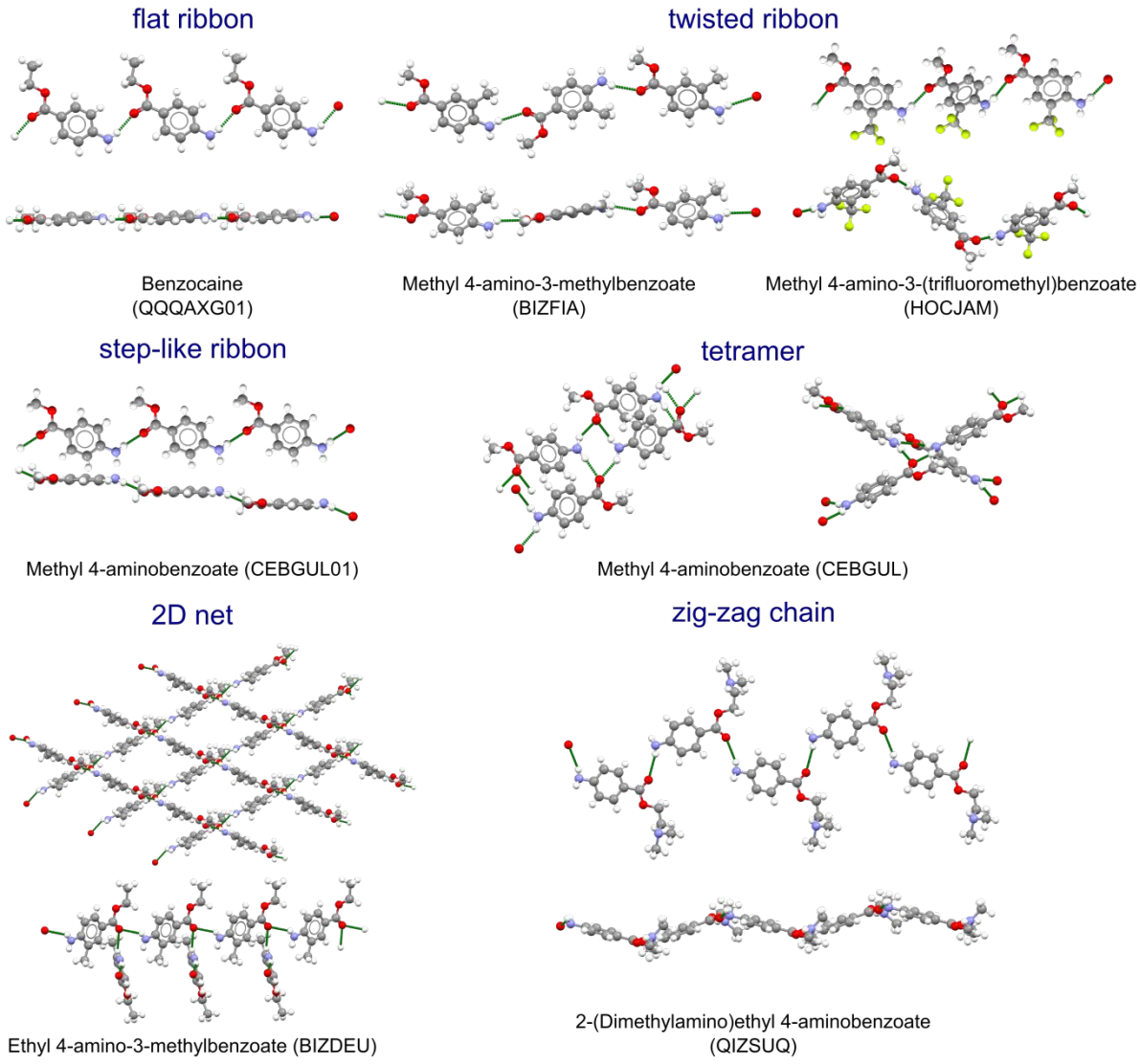

Figure S15 Different types of motives formed by N-H···O bonder esters of 4-aminobenzoic acid and its derivatives.

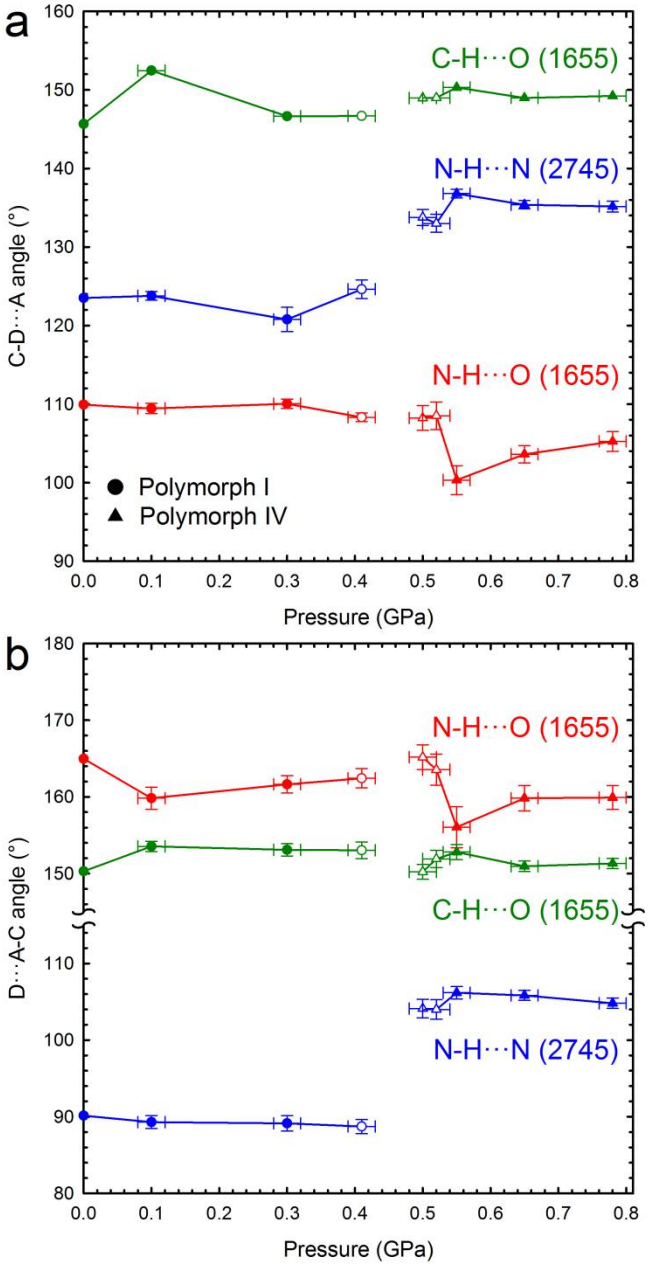

Figure S16 Pressure dependence of (a) C-D···A and (b) D···A-C Donohue angles (Katrusiak, 2003) for N-H···O, N-H···N and C-H···O contacts in crystals of BZC polymorphs I (circles) and IV (triangles), shown in red, blue and green, respectively. Data for samples obtained from MeOH:EtOH:H_2O 16:3:1 vol. solution is marked with full symbols, while open symbols mark data collected with the use of DMSO. The ORTEP symmetry codes are explained in Table S2 in Supporting Information.

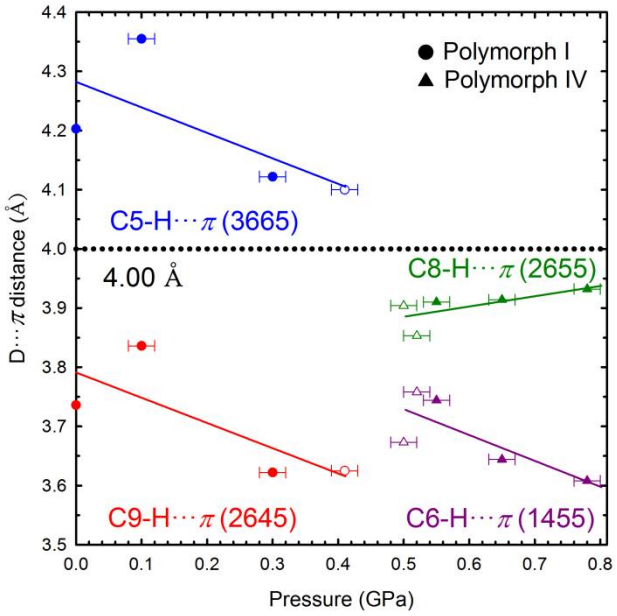

Figure S17 Pressure dependence of D··· π distances for C-H···π contacts in crystals of BZC polymorphs I (circles) and IV (triangles). The limit distance value used for determination of existing contacts is marked with dotted lines (Brandl *et al.*, 2001). Data for samples obtained from MeOH:EtOH:H_2O 16:3:1 vol. solution are marked with full symbols, while open symbols mark data collected with the use of DMSO. The ORTEP symmetry codes are explained in Table S2 in Supporting Information.

S2. Tables

S2.1 Crystallographic details

Table S1 Experimental details

Polymorph	**I**	**I**	**I**	**II**
Chemical formula	$C_9H_{11}NO_2$	$C_9H_{11}NO_2$	$C_9H_{11}NO_2$	$C_9H_{11}NO_2$
M_r (g·mol^{-1})	165.19	165.19	165.19	165.19
Crystal system	Monoclinic	Monoclinic	Monoclinic	Monoclinic
Space group	$P2_1/c$	$P2_1/c$	$P2_1/c$	$P2_1/c$
Pressure (GPa)	0.10(2)	0.30(2)	0.41(2)	0.50(2)
Temperature (K)	298(2)	298(2)	298(2)	298(2)
Unit-cell dimensions (Å, °)				
a	8.1928(6)	8.24(3)	8.171(13)	6.3608(8)
b	5.4539(5)	5.4015(9)	5.3995(9)	5.1830(7)
c	20.07(5)	19.519(3)	19.515(3)	24.75(5)
β	91.47(4)	91.55(6)	92.00(4)	96.66(5)
Volume (Å^3)	896(2)	868(3)	860.4(14)	810.4(17)
Z	4	4	4	4
D_x (g·cm^{-3})	1.224	1.264	1.275	1.354
Radiation type,	MoK_α	MoK_α	MoK_α	MoK_α
Absorption coefficient μ (mm^{-1})	0.087	0.090	0.091	0.096
Crystal size (mm)	0.43x0.1x0.1	0.44x0.44x0.10	0.34x0.29x0.10	0.34x0.31x0.10
Crystal colour	Colourless	Colourless	Colourless	Colourless
Hydrostatic medium	MeOH:EtOH:H_2O	MeOH:EtOH:H_2O	DMSO	DMSO
Diffractometer	Xcalibur, Eos			
F(000) (e)	352	352	352	352
2θ max (°)	53.94	53.64	53.87	53.97
Min./Max. indices h	-10/10	-1/1	-2/2	-8/8
k	-6/6	-6/6	-6/6	-6/6
l	-4/4	-23/24	-24/24	-6/6
Reflections collected/unique	442/442	2925/292	3571/462	3446/396
R_{int}	0.0989	0.0382	0.0690	0.1463
(sin $\theta/\lambda)_{max}$ (Å^{-1})	0.638	0.635	0.637	0.638
Observed reflections (I>4σ_I)	238	197	228	197
Data/parameters/restraints	442/100/123	292/99/132	462/99/133	396/99/141
Goodness of fit on F^2	1.000	1.163	1.102	1.157
Final R_1/wR_2 indices (I>4σ_I)	0.0610/0.1485	0.0438/0.1085	0.0867/0.2331	0.0910/0.2073
R_1/wR_2 indices (all data)	0.1218/0.1681	0.0730/0.1308	0.1521/0.2772	0.1703/0.2603
H-atom treatment	H-atom parameters constrained			
$\Delta\rho_{max}$, $\Delta\rho_{min}$ (eÅ^{-3})	0.086, -0.070	0.054, -0.093	0.136, -0.150	0.174, -0.166
Weighting scheme[a]: x; y	0.1127, 0	0.0682, 0.2839	0.1481, 0	0.125, 0.275
Extinction coefficient	–	–	–	–
Absorption corrections	none	multi-scan	multi-scan	multi-scan
Sample transmission min/max	-/ -	0.65/ 1.00	0.53/ 1.00	0.61/ 1.00
Computer programs	CrysAlis PRO 1.171.38.41 (Rigaku OD, 2015), SHELXS (Sheldrick, 2008), SHELXL (Sheldrick, 2015), Olex2 (Dolomanov *et al.*, 2009).			

Table S1 Experimental details- *continuation*

Polymorph	**II**	**II**	**II**	**II**
Chemical formula	$C_9H_{11}NO_2$	$C_9H_{11}NO_2$	$C_9H_{11}NO_2$	$C_9H_{11}NO_2$
M_r (g·mol^{-1})	165.19	165.19	165.19	165.19
Crystal system	Monoclinic	Monoclinic	Monoclinic	Monoclinic
Space group	$P2_1/c$	$P2_1/c$	$P2_1/c$	$P2_1/c$
Pressure (GPa)	0.52(2)	0.55(2)	0.65(2)	0.78(2)
Temperature (K)	298(2)	298(2)	298(2)	298(2)
Unit-cell dimensions (Å, °)				
a	6.3399(8)	6.3050(10)	6.3679(8)	6.3410(7)
b	5.1789(6)	5.1839(4)	5.1671(6)	5.1594(5)
c	24.80(7)	24.94(8)	24.58(8)	24.52(6)
β	96.58(6)	96.25(8)	96.25(6)	96.05(5)
Volume (Å^3)	809(2)	810(3)	804(3)	798(2)
Z	4	4	4	4
D_x (g·cm^{-3})	1.356	1.354	1.365	1.375
Radiation type,	MoK_α	MoK_α	MoK_α	MoK_α

Absorption coefficient μ (mm^{-1})	0.096	0.096	0.0492	0.098
Crystal size (mm)	0.47x0.31x0.10	0.42x0.34x0.10	0.43x0.31x0.10	0.43x0.31x0.10
Crystal colour	Colourless	Colourless	Colourless	Colourless
Hydrostatic medium	DMSO	MeOH:EtOH:H_2O	MeOH:EtOH:H_2O	MeOH:EtOH:H_2O
Diffractometer	Xcalibur, Eos			
F(000) (e)	352	352	352	352
2θ max (°)	51.87	52.95	53.09	53.00
Min./Max. indices h	-7/8	-7/7	-7/8	-7/7
k	-6/6	-6/6	-6/6	-6/6
l	-6/6	-6/6	-5/5	-5/5
Reflections collected/unique	2846/328	2490/270	2457/296	2437/289
R_{int}	0.1179	0.0518	0.0492	0.0536
$(\sin\theta/\lambda)_{max}$ (Å^{-1})	0.615	0.627	0.629	0.628
Observed reflections (I>4σ_I)	209	225	223	224
Data/parameters/restraints	328/99/134	270/99/125	296/99/142	289/111/132
Goodness of fit on F^2	1.164	1.062	1.164	1.076
Final R_1/wR_2 indices (I>4σ_I)	0.0931/0.2298	0.0627/0.1584	0.0435/0.0970	0.0426/0.1053
R_1/wR_2 indices (all data)	0.1348/0.2797	0.0712/0.1717	0.0626/0.1044	0.0615/0.1209
H-atom treatment	H-atom parameters constrained			
$\Delta\rho_{max}$, $\Delta\rho_{min}$ (eÅ^{-3})	0.178, -0.143	0.113, -0.105	0.083, -0.081	0.075, -0.082
Weighting scheme[a]: x; y	0.164, 0.695	0.1321, 0.4918	0.0471, 0.3983	0.0968, 0
Extinction coefficient	–	–	–	–
Absorption corrections	multi-scan	multi-scan	multi-scan	multi-scan
Sample transmission min/max	0.41/ 1.00	0.11/ 1.00	0.05/ 1.00	0.02/ 1.00
Computer programs	CrysAlis PRO 1.171.38.41 (Rigaku OD, 2015), SHELXS (Sheldrick, 2008), SHELXL (Sheldrick, 2015), Olex2 (Dolomanov *et al.*, 2009).			

S2.2 Intermolecular contacts geometry

Table S2 The ORTEP symmetry codes (Farrugia, 2012)

ORTEP code	Symmetry operation
1455	x-1, y, z
1655	x+1, y, z
2645	-x+1, -0.5+y, 0.5-z
2655	-x+1, 0.5+y, 0.5-z
2745	-x+2, -0.5+y, 0.5-z
3655	-x+1, -y, -z

Table S3 The geometry of D-H···A contacts in polymorphs I and IV

Polymorph		**I**[a]	**I**	**I**	**I**	**II**	**II**	**II**	**II**	**II**
	p (GPa)	0.0001	0.10(2)	0.30(2)	0.41(2)	0.50(2)	0.52(2)	0.55(2)	0.65(2)	0.78(2)
	H-bond									
N-H···O (1655)	N···O (Å)	2.956	2.957(16)	2.89(3)	2.908(22)	3.05(3)	3.06(4)	3.20(4)	3.09(2)	3.05(2)
	H···O (Å)	2.105	2.101	2.171	2.099	2.186	2.202	2.340	2.228	2.241
	N-H···O (°)	168.2	160.4	136.5	152.7	176.3	171.3	173.0	172.0	158.3
	C-N···O (°)	109.9	109.4(6)	110.0(6)	108.3(6)	108.2(16)	108.5(18)	100.3(18)	103.6(11)	105.2(13)
	N···O-C (°)	165.0	159.8(15)	161.6(11)	162.4(13)	165.2(16)	163.5(20)	156.1(27)	159.8(17)	159.9(15)
	N···N (Å)	3.316	3.31(2)	3.258(9)	3.278(11)	3.57(4)	3.560(4)	3.39(4)	3.46(3)	3.50(3)
	H···N (Å)	2.426	2.620	2.440	2.542	2.943	2.890	2.805	2.894	3.021

C-H···O (1655)N-H···N (2745)	N-H···N (°)	165.3	135.0	154.2	141.6	131.4	135.5	125.7	124.8	117.2
	C-N···N (°)	123.5	123.8 (5)	120.8(15)	124.6(12)	133.8(10)	133.0(11)	136.8(6)	135.4(5)	135.2(7)
	N···N-C (°)	90.1	89.3(8)	89.1(10)	88.7(9)	104.1(12)	104.0(13)	106.2(8)	105.8(7)	104.8(7)
	C···O (Å)	3.491	3.425(6)	3.40(3)	3.339(21)	3.453(8)	3.448(8)	3.422(6)	3.428(4)	3.413(6)
	H···O (Å)	2.746	2.696	2.668	2.612	2.700	2.694	2.655	2.674	2.662
	C-H···O (°)	134.34	135.8	135.6	135.4	138.7	138.7	140.3	138.7	138.4
	Ctr-C···O[b] (°)	145.7	152.5	146.6	146.7	149.0	149.0	150.3	149.0	149.2
	C···O-C (°)	150.3	153.6(7)	153.1(8)	153.0(11)	150.2(10)	151.9(11)	152.8(10)	151.0(7)	151.3(7)

[a] Based on previously-reported structure: Refcode QQQAXG04 (Chan *et al.*, 2009).

[b] Due to the donor (carbon atom) of the H-bond being part of the aromatic ring, the X-D···A angle was calculated using the position of the aromatic ring centroid (X=Ctr) determined with program Mercury (Bruno *et al.*, 2002).

Table S4 The geometry of D-H···π contacts in polymorphs I and IV.

Polymorph		I[a]	I	I	I	II	II	II	II	II
p (GPa)		0.0001	0.10(2)	0.30(2)	0.41(2)	0.50(2)	0.52(2)	0.55(2)	0.65(2)	0.78(2)
contact										
N-H···O (1655) C5-H5··· π (3665) C-H···O (1655)	C···π (Å)	4.203	4.355	4.122	4.100					
	H··· π (Å)	3.487	3.336	3.428	3.405					
	C-H··· π (°)	134.1	130.5	133.4	133.3					
N-H···O (1655) C9-H9··· π (2645) C-H···O (1655)	C···π (Å)	3.736	3.836	3.622	3.625					
	H··· π (Å)	2.823	2.882	2.759	2.699					
	C-H··· π (°)	152.6	172.9	149.6	162.7					
C6-H6··· π	C···π (Å)					3.904	3.853	3.910	3.914	3.932
	H··· π (Å)					3.277	3.230	3.280	3.284	3.306

C8-H8···π (2655) (1455)	C-H··· π (°)		126.6	126.1	127.0	126.8	126.7
	C···π (Å)		3.673	3.758	3.744	3.644	3.608
	H··· π (Å)		2.784	2.911	2.904	2.759	2.726
	C-H··· π (°)		152.5	146.4	145.7	151.9	151.5

Table S5 Primary motifs and directions of their propagation in crystal structures of esters of 4-aminobenzoic acid and its derivatives deposited in CSD.

Refcode	Compound name	Primary motive	Propagation direction
BEWYIL	Procaine (novocaine)	Tetramer	-
BEWYIL01	Procaine (novocaine)	Tetramer	-
BIZDEU	Ethyl-4-amino-3-methylbenzoate	2D net(formed by N-H···O bonded ribbons)	[100]&[010]
BIZFIA	Methyl-4-amino-3-methylbenzoate	Twisted ribbon	[001]
CEBGUL	Methyl p-aminobenzoate	Tetramer	-
CEBGUL01	Methyl p-aminobenzoate	Ribbon	[100]
EZAVIK	4-aminobenzoic acid n-butyl ester	Ribbon	[100]
GANBEF	ethyl-4-amino-2,3,5,6-tetrafluorobenzoate	Ribbon	[010]
HOCJAM	Methyl-4-amino-3(trifluoromethyl)benzoate	Twisted ribbon	[001]
KUSKUF	4-methylbenzyl 4-aminobenzoate	Ribbon	[100]
QQQAXG01	Benzocaine (polymorph II)	Ribbon	[010]
QQQAXG02	Benzocaine (polymorph I)	Ribbon	[100]
QQQAXG03	Benzocaine (polymorph III)	Ribbon	[100]
QQQAXG04	Benzocaine (polymorph I)	Ribbon	[100]
QQQAXG05	Benzocaine (polymorph II)	Ribbon	[100]
QQQAXG00	Benzocaine (polymorph I)	Ribbon	[100]

QQQAXG10	Benzocaine (polymorph II)	Ribbon	[100]
SICQOK	Methyl-4-amino-3-methoxybenzoate	Tetramer	-
XEYJET	Ethyl 4-amino-3-trifluoromethylbenzoate	Tetramer	-
QIZSUQ	2-(dimethylamino)ethyl 4-aminobenzoate	Zig-zag chain	[010]

Table S6 Selected geometric parameters (Å,°)

a) Polymorph I at 0.10 GPa

O1—C7	1.210 (10)	C2—C1	1.3900
N1—C1	1.357 (8)	C1—C6	1.3900
C4—C3	1.3900	C6—C5	1.3900
C4—C5	1.3900	C7—O2	1.34 (2)
C4—C7	1.431 (11)	O2—C8	1.44 (2)
C3—C2	1.3900	C8—C9	1.55 (3)
C3—C4—C5	120.0	C5—C6—C1	120.0
C3—C4—C7	121.5 (7)	C6—C5—C4	120.0
C5—C4—C7	118.5 (7)	O1—C7—C4	128.7 (12)
C2—C3—C4	120.0	O1—C7—O2	117.2 (11)
C3—C2—C1	120.0	O2—C7—C4	113.9 (9)
N1—C1—C2	119.5 (5)	C7—O2—C8	118.6 (13)
N1—C1—C6	120.5 (5)	O2—C8—C9	108.2 (13)
C2—C1—C6	120.0		

b) Polymorph I at 0.30 GPa

O1—C7	1.22 (2)	C4—C3	1.3900
C1—C6	1.3900	C4—C7	1.501 (8)
C1—C2	1.3900	C3—C2	1.3900
C1—N1	1.39 (2)	O2—C8	1.45 (3)
C6—C5	1.3900	O2—C7	1.351 (11)
C5—C4	1.3900	C8—C9	1.513 (13)
C6—C1—C2	120.0	C2—C3—C4	120.0
C6—C1—N1	122.0 (8)	C3—C2—C1	120.0
C2—C1—N1	118.0 (8)	C7—O2—C8	116.8 (18)
C1—C6—C5	120.0	O2—C8—C9	107.5 (19)
C4—C5—C6	120.0	O1—C7—C4	128.2 (10)
C5—C4—C3	120.0	O1—C7—O2	119.5 (15)
C5—C4—C7	117.6 (6)	O2—C7—C4	112.2 (13)
C3—C4—C7	122.3 (6)		

c) Polymorph I at 0.41 GPa

O1—C7	1.22 (3)	C4—C7	1.501 (19)
O2—C7	1.346 (14)	C3—C2	1.3900
O2—C8	1.47 (3)	C2—C1	1.3900
N1—C1	1.330 (19)	C1—C6	1.3900
C4—C3	1.3900	C6—C5	1.3900
C4—C5	1.3900	C9—C8	1.524 (12)

C7—O2—C8	113.4 (18)	C2—C1—C6	120.0
C3—C4—C5	120.0	C5—C6—C1	120.0
C3—C4—C7	121.7 (7)	C6—C5—C4	120.0
C5—C4—C7	118.3 (7)	O1—C7—O2	122.9 (19)
C4—C3—C2	120.0	O1—C7—C4	127.3 (12)
C3—C2—C1	120.0	O2—C7—C4	109.8 (16)
N1—C1—C2	120.1 (7)	O2—C8—C9	107.1 (17)
N1—C1—C6	119.9 (7)		

d) Polymorph IV at 0.50 GPa

O1—C7	1.222 (16)	C4—C7	1.500 (2)
O2—C7	1.30 (2)	C5—C6	1.3900
O2—C8	1.436 (17)	C6—C1	1.3900
N1—C1	1.374 (13)	C1—C2	1.3900
C4—C5	1.3900	C2—C3	1.3900
C4—C3	1.3900	C8—C9	1.50 (3)
C7—O2—C8	115.9 (10)	C6—C1—C2	120.0
C5—C4—C3	120.0	C3—C2—C1	120.0
C5—C4—C7	120.0 (7)	C2—C3—C4	120.0
C3—C4—C7	119.7 (7)	O1—C7—O2	124.6 (9)
C4—C5—C6	120.0	O1—C7—C4	120.8 (14)
C1—C6—C5	120.0	O2—C7—C4	114.3 (10)
N1—C1—C6	120.5 (11)	O2—C8—C9	105.7 (10)
N1—C1—C2	119.4 (11)		

e) Polymorph IV at 0.52 GPa

O1—C7	1.181 (17)	C4—C7	1.500 (3)
O2—C7	1.31 (2)	C5—C6	1.3900
O2—C8	1.51 (2)	C6—C1	1.3900
N1—C1	1.351 (14)	C1—C2	1.3900
C4—C5	1.3900	C2—C3	1.3900
C4—C3	1.3900	C8—C9	1.49 (3)
C7—O2—C8	118.5 (9)	C6—C1—C2	120.0
C5—C4—C3	120.0	C3—C2—C1	120.0
C5—C4—C7	119.7 (7)	C2—C3—C4	120.0
C3—C4—C7	120.2 (7)	O1—C7—O2	123.7 (11)
C6—C5—C4	120.0	O1—C7—C4	123.0 (15)
C5—C6—C1	120.0	O2—C7—C4	113.0 (9)
N1—C1—C6	120.4 (12)	C9—C8—O2	107.2 (10)
N1—C1—C2	119.4 (12)		

f) Polymorph IV at 0.55 GPa

O1—C7	1.199 (13)	C4—C7	1.487 (16)
O2—C7	1.31 (3)	C5—C6	1.3900
O2—C8	1.47 (2)	C6—C1	1.3900
N1—C1	1.422 (19)	C1—C2	1.3900
C4—C5	1.3900	C2—C3	1.3900
C4—C3	1.3900	C8—C9	1.45 (3)
C7—O2—C8	118.8 (9)	C2—C1—N1	123.4 (11)
C5—C4—C3	120.0	C3—C2—C1	120.0
C5—C4—C7	119.7 (8)	C2—C3—C4	120.0
C3—C4—C7	120.2 (9)	O1—C7—O2	120.8 (18)
C4—C5—C6	120.0	O1—C7—C4	124 (2)
C1—C6—C5	120.0	O2—C7—C4	114.8 (8)
C6—C1—N1	116.6 (11)	C9—C8—O2	107.2 (9)
C6—C1—C2	120.0		

g) Polymorph IV at 0.65 GPa

O1—C7	1.221 (11)	C4—C7	1.481 (10)
O2—C7	1.313 (19)	C5—C6	1.3900
O2—C8	1.460 (11)	C6—C1	1.3900
N1—C1	1.425 (10)	C1—C2	1.3900
C4—C5	1.3900	C2—C3	1.3900
C4—C3	1.3900	C8—C9	1.54 (2)
C7—O2—C8	116.4 (6)	C2—C1—N1	122.1 (7)
C5—C4—C3	120.0	C1—C2—C3	120.0
C5—C4—C7	118.6 (6)	C2—C3—C4	120.0
C3—C4—C7	121.3 (7)	O1—C7—O2	122.4 (11)
C4—C5—C6	120.0	O1—C7—C4	124.3 (15)
C1—C6—C5	120.0	O2—C7—C4	113.3 (7)
C6—C1—N1	117.9 (7)	O2—C8—C9	106.7 (6)
C6—C1—C2	120.0		

h) Polymorph IV at 0.78 GPa

O2—C7	1.322 (19)	C4—C3	1.375 (10)
O2—C8	1.446 (12)	C2—C3	1.375 (11)
O1—C7	1.221 (10)	C2—C1	1.40 (2)
N1—C1	1.396 (12)	C5—C6	1.373 (12)
C4—C7	1.447 (12)	C6—C1	1.379 (12)
C4—C5	1.41 (2)	C8—C9	1.53 (2)
C7—O2—C8	116.6 (6)	C6—C5—C4	121.0 (9)
C5—C4—C7	118.6 (8)	C5—C6—C1	121.4 (13)

C3—C4—C7	124.5 (12)	C4—C3—C2	122.6 (11)
C3—C4—C5	116.8 (8)	O2—C8—C9	106.7 (6)
C3—C2—C1	119.9 (8)	N1—C1—C2	121.1 (10)
O2—C7—C4	112.6 (8)	C6—C1—N1	120.9 (14)
O1—C7—O2	121.9 (11)	C6—C1—C2	118.0 (8)
O1—C7—C4	125.5 (15)		

References

Arunan, E., Desiraju, G. R., Klein, R. A., Sadlej, J., Scheiner, S., Alkorta, I., Clary, D. C., Crabtree, R. H., Dannenberg, J. J., Hobza, P., Kjaergaard, H. G., Legon, A. C., Mennucci, B. & Nesbitt, D. J. (2011). *Pure Appl. Chem.* **83**, 1637–1641.

Brandl, M., Weiss, M. S., Jabs, A., Sühnel, J. & Hilgenfeld, R. (2001). *J. Mol. Biol.* **307**, 357–377.

Bruno, I. J., Cole, J. C., Edgington, P. R., Kessler, M., Macrae, C. F., McCabe, P., Pearson, J. & Taylor, R. (2002). *Acta Crystallogr. B.* **58**, 389–397.

Chan, E. J., Rae, A. D. & Welberry, T. R. (2009). *Acta Crystallogr. B.* **65**, 509–515.

Farrugia, L. J. (2012). *J. Appl. Crystallogr.* **45**, 849–854.

Katrusiak, A. (2003). *Crystallogr. Rev.* 9, 91–133.